Journal of Macromolecular Science, Part A
Publication details, including instructions for authors and subscription information:
http://www.informaworld.com/smpp/title~content=t713597274

Forced Oscillations in a Nonisothermal Continuous Polymerization Reactor

D. Konopnicki[ab]; J. L. Kuester[a]
[a] Arizona State University, Tempe, Arizona [b] Texaco, Inc., Bellaire, Texas

To cite this Article Konopnicki, D. and Kuester, J. L.(1974) 'Forced Oscillations in a Nonisothermal Continuous Polymerization Reactor', Journal of Macromolecular Science, Part A, 8: 5, 887 — 908
To link to this Article: DOI: 10.1080/00222337408066406
URL: http://dx.doi.org/10.1080/00222337408066406

J. MACROMOL. SCI.—CHEM., A8(5), pp. 887-908 (1974)

Forced Oscillations in a Nonisothermal Continuous Polymerization Reactor*

D. KONOPNICKI† and J. L. KUESTER

Arizona State University
Tempe, Arizona 85281

ABSTRACT

A dynamic model of a nonisothermal continuous stirred tank polymerization reactor is developed to predict product molecular weight distribution parameters. Deliberate oscillations in operating variables were programmed into the model and the resulting time-averaged reactor performance indices compared with that for optimum steady-state operation. Results indicate that periodic operation does influence polymerization reactor performance, particularly with regard to time-averaged molecular weight polydispersity. Significant resonant behavior was encountered with molecular weight properties at low frequencies.

INTRODUCTION

Continuous polymerization reactors are usually operated in a steady-state mode, i.e., the operating variables are held constant.

*Presented in part at the 1973 Summer Simulation Conference, Montreal, July 1973.

†Present address: Texaco, Inc., Bellaire, Texas 77401.

There is evidence in the recent literature, however, that reactor performance might be improved with forced oscillations in control variables. Thus a polymer product could conceivably be produced in this manner that would not be possible with steady state operation.

Several studies have considered the effect of forced oscillations upon the performance of an isothermal continuously stirred tank polymerization reactor [1-4]. A narrowing of the molecular weight distribution has been claimed in model studies for a condensation system [1] and termination free "living polymer" system [2]. Also an experimental study has indicated a narrowing of the distribution is possible for a photoinitiated emulsion system [3]. Broadening of the distribution has been achieved in model studies for free radical addition systems with combination termination [1, 4] and a simple addition system without termination [4]. Polydispersity, the ratio of weight-average molecular weight (M_w) to number-average molecular weight (M_n), was used as an indication of the distribution breadth in all cases.

Nonisothermal polymerization model developments have been rare. Mathematically, all that is added to the equation system is an energy balance. However, in an iterative numerical solution scheme, the addition of the usual Arrhenius-type exponential temperature functions can create havoc with numerical model solution schemes. Isothermal operation is an ideal concept however, and few commercial polymerization reactor systems operate in this manner. Due to exponential dependence, changes in temperature can have very large effects on production rate and molecular weight distributions.

Most previous polymerization models have used conventional kinetics which does not account for the viscous effects of the solution on the polymerization rates. As the polymerization proceeds, the medium becomes more viscous, and the rate of polymerization increases. This effect is explained by the difficulty in bringing together two reacting chains in a viscous solution; thus the termination rate constant decreases as the viscosity of the solution increases. The initiator efficiency also decreases with increasing viscosity because more initiated radicals terminate with each other rather than react with monomer molecules. This phenomenon, known as the "Trommsdorff effect" or "autoacceleration," generally becomes significant at conversions of 20% or more [5].

The objective of the work reported in this paper was to establish the effect of periodic operation upon the time-averaged molecular weight distribution of a polymer which is produced in a nonisothermal continuously stirred tank reactor (CSTR). Due to the availability of kinetic data [6], the particular system chosen for study was the polymerization of styrene in toluene solvent using azobisisobutyronitrile as the initiator. The major extensions of earlier work included the following:

(1) Nonisothermal operation.
(2) Inclusion of viscosity effects on the initiator efficiency and termination rate constant.
(3) A check on the validity of the pseudosteady-state assumption (PSSA).
(4) A broad scan of steady-state optimization problem base conditions.
(5) Alternate forcing function forms and combinations.

DEVELOPMENT OF THE SYSTEM EQUATIONS

The free radical mechanism and literature values for the various rate constants are summarized in Table 1.

TABLE 1. Free Radical Polymerization Mechanism [6]

Initiation: $I + 2M \xrightarrow{k_i} 2R_1$

Propagation: $R_n + M \xrightarrow{k_p} R_{n+1}$

Chain transfer

to solvent: $R_n + S \xrightarrow{k_{fs}} P_n + S\cdot$

to monomer: $R_n + M \xrightarrow{k_{fm}} P_n + M\cdot$

Termination

combination: $R_n + R_m \xrightarrow{k_t} P_{n+m}$

disproportionation: $R_n + R_m \xrightarrow{k_{td}} P_n + P_m$

where $n,m = 1, 2, 3, \ldots, \infty$.

$k_i = 9.48 \times 10^{16} \exp(-15{,}000/T)$
$k_p = 6.30 \times 10^{8} \exp(-3557/T)$
$k_{t,i} = 7.53 \times 10^{10} \exp(-844/T)$
$k_{td} = 0.0$
$k_{fs} = 3.54 \times 10^{10} \exp(-8660/T)$
$k_{fm} = 1.385 \times 10^{8} \exp(-6377/T)$

To develop the conservation equations for the system, the following assumptions were made:

(1) Concentrations equal activities.
(2) Reaction rate constants are independent of chain length except the termination rate constant.
(3) All reactions are elementary except the initiation reaction.
(4) All reactions are homogeneous.
(5) All activities of $M\cdot$, $S\cdot$, and R_1 are equal.
(6) The reactions are irreversible.
(7) The reactor contents are perfectly mixed.
(8) The inlet polymer concentrations are assumed to be zero.
(9) The solvent concentration is constant.
(10) The heat of reaction contribution from the propagation step dominates and can be considered constant.
(11) The mixture heat capacity can be approximated at the inlet conditions.

TABLE 2. Conservation Equation Summary

Component mass balances:

$$dI/dt = I^\circ/\theta - k_i I - I/\theta$$

$$dM/dt = M^\circ/\theta - M/\theta - k_p M R_T - 2k_i f I - k_{fm} M R_T$$

$$dR_1/dt = -R_{1/\theta} + 2k_i f I - k_p R_1 M - k_t R_1 R_T + k_{fs} S R_T + k_{fm} M R_T - k_{fs} R_1 S - k_{fm} M R_1$$

$$dR_n/dt = -R_{n/\theta} - k_p R_n M + k_p R_{n-1} M - k_t R_n R_T - k_{fs} S R_n - k_{fm} R_n M$$

$$dP_n/dt = -P_{n/\theta} + \frac{1}{2} k_t \sum_{m=1}^{n-1} R_m R_{n-m} + k_{fs} R_n S + k_{fm} M R_n$$

where $n,m = 1, 2, 3, \ldots, \infty$

Energy balance:

$$dT/dt = [v_T(S^\circ C_{p,s} + M^\circ C_{p,M})(T^\circ - T) - \bar{U}A\,(T - T_j) - V \Delta H_{rxn,p} k_p M \sum_{n=1}^{\infty} R_n]/[V(S^\circ C_{p,s} + M^\circ C_{p,m})]$$

Utilizing these assumptions, the component mass balances for initiator (I), monomer (M), live polymer species (R_n), and dead polymer species (P_n) and energy balance can be developed as summarized in Table 2. In Table 2, θ is the residence time, f is the initiator efficiency factor [6], t is time, T is temperature, v_T is volumetric flow rate, and C_p is heat capacity. The zero subscript indicates inlet conditions.

The equation set summarized in Table 2 represents an infinite set of coupled, nonlinear ordinary differential equations. To avoid the formidable task of attempting a direct solution over the range of significant polymer concentrations, an alternate approach is to reformulate the conservation equations in terms of the leading moments of the polymer distribution. The net result will be to reduce the infinite set of equations to a finite set from which the number-average and weight-average molecular weights can be calculated.

A direct and efficient method of obtaining moment equations from the equations of Table 2 is by use of Z-transforms [7]. Pertinent properties of Z-transforms in terms of the live polymer species concentrations, R_n, and live moments, λ_k, are given in Table 3. Similar expressions can be developed in terms of the dead species concentrations, P_n, and dead moments, σ_k.

Applying Z-transform theory to the live and dead polymer species equations of Table 2, the infinite equation sets are reduced to six equations for the leading live and dead moments (Table 4).

The total moments, σ_k, for the complete distribution are obtained by adding the corresponding live and dead moments,

TABLE 3. Z-Transform Theory

Z-transform:	$\bar{R}(z,t) = \sum_{n=1}^{\infty} R_n(t) z^{-n}$
Moment generation theorem:	$\lambda_k = \left(-z \frac{d}{dz}\right)^k \bar{R}(z,t)\Big\|_{z=1}$
Shift theorem:	$z[R(n-k)] = z^{-k}\bar{R}(z)$
Real convolution theorem:	$z\left[\sum_{n=1}^{n} R_1(n)\, R_2(n-k)\right] = \bar{R}_1(z)\bar{R}_2(z)$

TABLE 4. Moment Equations

Live moments:

$$d\lambda_0/dt = -\lambda_0/\theta + 2k_i fI - k_t\lambda_0^2$$

$$d\lambda_1/dt = \lambda_1/\theta + 2k_i fI + k_p M\lambda_0 - k_t\lambda_0\lambda_1 - k_{fs}S\lambda_1 - k_{fm}M\lambda_1 + k_{fs}S\lambda_0 + k_{fm}M\lambda_0$$

$$d\lambda_2/dt = \lambda_1/\theta - \lambda_2/\theta + 2k_i fI + 2k_p M\lambda_1 + k_p M\lambda_0 + k_t\lambda_0\lambda_1 - k_t\lambda_0\lambda_2 + k_{fs}S\lambda_1 - k_{fs}S\lambda_2 + k_{fm}M\lambda_1 - k_{fm}M\lambda_1 + k_{fs}S\lambda_0 + k_{fm}M\lambda_0$$

Dead moments:

$$d\mu_0/dt = -\mu_0/\theta + \lambda_0(\frac{1}{2}k_t\lambda_0 + k_{fs}S + k_{fm}M)$$

$$d\mu_1/dt = -\mu_1/\theta + \lambda_1(k_t\lambda_0 + k_{fs}S + k_{fm}M)$$

$$d\mu_2/dt = -\mu_2/\theta + \mu_1/\theta - \lambda_1(k_t\lambda_0 - k_t\lambda_1 + k_{fs}S + k_{fm}M) + \lambda_2(k_t\lambda_0 + k_{fs}S + k_{fm}M)$$

$$\sigma_0 = \lambda_0 + \mu_0 \quad (1)$$

$$\sigma_1 = \lambda_1 + \mu_1 \quad (2)$$

$$\sigma_2 = \lambda_2 + \mu_2 \quad (3)$$

The number-average chain length, r_n, weight-average chain length, r_w, and polydispersity, M_w/M_n, are then obtained from the total moments,

$$r_n = \sigma_1/\sigma_0 \tag{4}$$

$$r_w = \sigma_2/\sigma_1 \tag{5}$$

$$M_w/M_n = r_w/r_n \tag{6}$$

Number- and weight-average molecular weights are obtained by multiplying the average degree of polymerization by the repeat unit molecular weight.

The pseudosteady-state assumption can be applied to the above equations by setting the live moment derivatives equal to zero, i.e.,

$$d\lambda_0/dt = d\lambda_1/dt = d\lambda_2/dt = 0 \tag{7}$$

The energy balance as presented in Table 2 is converted in terms of moments by noting the following,

$$\sum_{n=1}^{\infty} R_n = \lambda_0 \tag{8}$$

To complete the model development, relationships are needed to account for viscosity effects on the initiator efficiency and termination rate constants. To adequately predict the rates of polymerization in a viscous medium, attempts have been made to apply the theory of diffusion-controlled polymerization reactions, but insufficient kinetic data made this approach infeasible. Hui [5] has developed an empirical equation set relating viscosity, μ, to the termination rate constant, k_t, and to the initiator efficiency, f, for the polymerization of styrene in toluene solution. The solution viscosity was assumed to be a function of temperature, T, solvent concentration, S, polymer weight fraction, P_F, and number-average degree of polymerization, r_n. A nonlinear regression analysis was used to determine the empirical equation relating the above variables. The results are summarized in Table 5. The quantities $k_{t,i}$ and f_i are the termination rate constant and initiator efficiency at zero conversion, respectively [5].

TABLE 5. Viscosity Corrections [5]

$\log(\mu) = 17.66 - 0.311\log(1+S) - 7.72\log(T) - 10.23\log(1-P_F) - 11.82[\log(1-P_F)]^2 - 11.22[\log(1-P_F)]^3 + 0.839\log(r_n)$
$\log(k_t/k_{t,i}) = -0.133\log(1+\mu) - 0.0777[\log(1+\mu)]^2$
$\log(f/f_i) = -0.133\log(1+\mu)$

The relationships are restricted to a maximum viscosity of 3000 cP, monomer conversions of less than 70%, and polymer chain lengths of less than 4000.

SOLUTION STRATEGY

To establish the effect of periodic operation on reactor performance, the optimum steady-state performance is compared with the forced dynamic behavior. Thus the solution to two types of models are required: 1) steady-state CSTR, and 2) unsteady-state CSTR.

The equation system consists of a set of nine coupled, nonlinear equations involving the variables I, M, T, λ_0, λ_1, λ_2, μ_0, μ_1, and μ_2. The algebraic set for the steady-state case was solved utilizing the technique of Marquardt [8, 9] while the first-order ordinary differential equation system in time for the unsteady-state case was solved using a fourth-order Adams-Moulton predictor-corrector scheme [10, 11].

A single loop procedure was used for the unsteady-state general case while a two loop method was utilized for the other two systems. The single loop procedure consists of a direct simultaneous solution of the system equations at a sequence of time increments. The two loop procedures are more complicated. In the outer loop, values for I, M, T, μ_0, μ_1, and μ_2 are calculated using the predictor-corrector method. In the inner loop, an iterative procedure is used. Values of r_n and P_F from the previous time step are used to calculate values of λ_0, λ_1, λ_2, r_n, r_w, M_w/M_n, and P_F. Then the new values of r_n and P_F are used to again calculate λ_0, λ_1, λ_2, r_n, r_w, M_w/M_n, and P_F. Now the two different values of M_w/M_n are checked for convergence. If the difference between the two values is less than or equal to δ, the current values of λ_0, λ_1, λ_2, r_n, r_w, M_w/M_n, and P_F are accepted and the inner loop is completed for that particular time interval. Now the solution procedure returns to the outer loop where the value of the derivatives are calculated. These values are then used to compute I, M, T, μ_0, μ_1, and μ_2 at the next time interval to complete the outer loop.

The values of I, M, T, λ_0, λ_1, λ_2, μ_0, μ_1, and μ_2 are calculated as a function of time using the above unsteady-state methods. To calculate the time average conditions, values of I, M, T, λ_0, λ_1, λ_2, μ_0, μ_1, and μ_2 are stored in the computer memory at specified, equal intervals of time. The time average values of the stored variables are then computed by numerical intergration of

$$\bar{C}_i = \left[\int_{t_0}^{t_0+\Delta t} C_i \, dt\right] \Big/ \left[\int_{t_0}^{t_0+\Delta t} dt\right] \qquad (9)$$

This integration was done using Simpson's rule [10, 12].

OPTIMIZATION OF THE STEADY-STATE PERFORMANCE

To establish base conditions for the periodic studies, the steady-state CSTR model was optimized for various objective functions and constraints. The specific reactor conditions are summarized in Table 6. After scanning various reactor operating variables, the inlet initiator concentration and jacket temperature were deemed to be the most significant with regard to their effect on reactor performance (monomer conversion, average molecular weight, polydispersity.) The complex method [9, 13] constrained search technique was selected for the optimization. This method allows a function to be maximized or minimized subject to implicit and explicit constraints on the decision variables.

TABLE 6. Reactor Conditions

Solvent: Toluene
Monomer: Styrene
Initiator: Azobisisobutyronitrile
Inlet solvent concentration: 2.045 g moles/liter
Inlet monomer concentration: 7.325 g moles/liter
Inlet temperature: 298°K
Residence time: 100 min
Total flow rate: 0.5 liters/min
Reactor volume: 50 liters
Reactor diameter: 1.058 ft
Reactor height: 2.00 ft
Heat transfer area: 6.66 ft^2
Heat transfer coefficient: 151 cal/min ft^2 °K
Heat capacity of solvent: 39.43 cal/g mole °K
Heat capacity of monomer: 46.50 cal/g mole °K
Heat of polymerization: -17,100 cal/g mole

TABLE 7. Steady-State Optimization (Case 1)

Objective function:	minimize M_w/M_n
Explicit constraints:	$0.001 \leq I^\circ \leq 0.1$ g moles/liter
	$298 \leq T_j \leq 385°K$
Implicit constraints:	$50 \leq$ % monomer conversion ≤ 100
	$500 \leq r_n \leq 10000$
Optimum values:	$T_j = 355°K$
	$I^\circ = 0.0224$ g moles/liter
	$r_n = 500$
	% monomer conversion = 50.4
	$M_w/M_n = 1.536$

TABLE 8. Steady-State Optimization (Case 2)

Objective function:	Maximize M_w/M_n
Explicit constraints:	$0.001 \leq I^\circ \leq 0.1$ g moles/liter
	$298 \leq T_j \leq 385°K$
Implicit constraints:	$50 \leq$ % monomer conversion ≤ 100
	$500 \leq r_n \leq 10000$
Optimum values:	$T_j = 384°K$
	$I^\circ = 0.0255$ g moles/liter
	$r_n = 605$
	% monomer conversion = 81.6
	$M_w/M_n = 1.690$

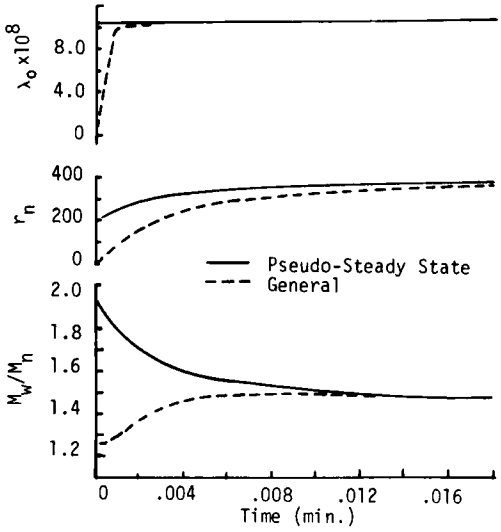

FIG. 1. Verification of the pseudosteady-state assumption (PSSA).

A number of optimization problems were posed, two of which are summarized in Tables 7 and 8. Both cases contain explicit constraints on the decision variables (initiator concentration, jacket temperature) and implicit constraints on the monomer conversion and number-average degree of polymerization. The objectives are to minimize and maximize the polydispersity subject to the constraints. The question of the desirability of narrow vs broad distribution is subject to controversy. For example, in many polymers a narrow distribution results in improved mechanical properties but relatively poor processing properties.

The results presented show a minimum M_w/M_n of 1.54 and a maximum of 1.69 subject to the common constraints for this particular system. The objective of forced oscillations in the decision variables is to produce a polymer with a smaller M_w/M_n for the first case or a larger M_w/M_n for the second case.

VERIFICATION OF THE PSEUDOSTEADY-STATE ASSUMPTION

Because of the controversy concerning the validity of the PSSA for the dynamic model, comparisons were made for the model with and without the assumption. The results are given in Fig. 1 where the total

TABLE 9. Periodic Operation Results (Sine Wave - Case 1)

Run	Variable	F(t)	r_n	Conversion	M_w/M_n
Opt.			500	50.4	1.536
1	I°	0.01 sin (0.01t)	596	49.8	1.551
2	I°	0.01 sin(0.1t)	492	49.8	1.565
3	I°	0.005 sin(0.01t)	499	50.3	1.540
4	I°	0.005 sin(0.1t)	499	50.3	1.544
5	T_j	10 sin(0.01t)	546	47.5	1.582
6	T_j	10 sin(0.1t)	497	50.6	1.568
7	T_j	20 sin(0.01t)	603	46.9	1.619
8	T_j	20 sin(0.1t)	489	50.9	1.636
9	I°	0.005 sin(0.01t)	490	46.3	1.641
	T_j	10 sin(0.01t + π)			
10	I°	0.005 sin(0.1t)	599	46.8	1.626
	T_j	20 sin(0.01t)			
11	I°	0.005 sin(0.01t)	495	50.6	1.569
	T_j	10 sin(0.1t)			
12	I°	0.005 sin(0.1t)	490	50.3	1.606
	T_j	20 sin(0.1t + π)			
13	I°	0.01 sin(0.1t)	489	46.3	1.666
	T_j	10 sin(0.01t + π)			
14	I°	0.01 sin(0.01t)	560	49.5	1.626
	T_j	20 sin(0.01t)			
15	I°	0.01 sin(0.1t)	474	49.3	1.645
	T_j	10 sin(0.1t)			
16	I°	0.01 sin(0.01t)	476	49.5	1.644
	T_j	20 sin(0.1t + π)			

TABLE 10. Periodic Operation Results (Square Wave - Case 1)

Run	Variable	F (t) Amp.	F (t) Period (min)	F (t) ϕ	r_n	Conversion	M_w/M_n
17	I°	±0.01	628		489	49.9	1.575
18	I°	±0.01	62.8		486	49.4	1.586
19	I°	±0.005	628		497	50.4	1.548
20	I°	±0.005	62.8		497	50.2	1.548
21	T_j	±10	628		584	47.0	1.584
22	T_j	±10	62.8		495	50.7	1.586
23	T_j	±20	628		634	49.0	1.657
24	T_j	±20	62.8		494	52.0	1.668
25	I°	±0.005	628		497	43.2	1.664
	T_j	±10	628	314			
26	I°	±0.005	62.8		627	48.8	1.667
	T_j	±20	628	0			
27	I°	±0.005	628		494	51.2	1.583
	T_j	±10	62.8	0			
28	I°	±0.005	62.8		494	50.9	1.631
	T_j	±20	62.8	31.4			
29	I°	±0.01	62.8		492	43.1	1.752
	T_j	±10	628	314			
30	I°	±0.01	628		552	52.9	1.679
	T_j	±20	628	0			
31	I°	±0.01	62.8		458	49.0	1.719
	T_j	±10	62.8	0			
32	I°	±0.01	628		464	49.9	1.707
	T_j	±20	62.8	31.4			

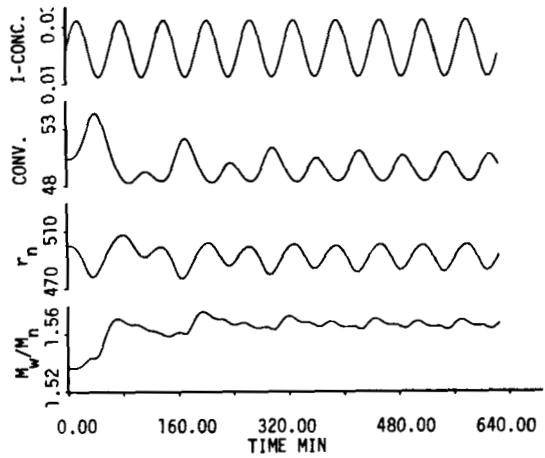

FIG. 2. Reactor dynamics (Run 2) for initiator concentration forcing function.

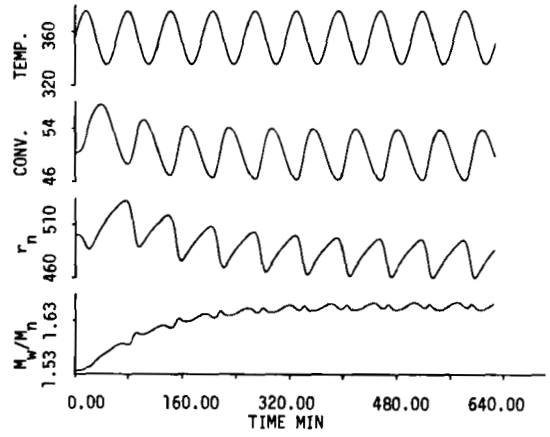

FIG. 3. Reactor dynamics (Run 8) for jacket temperature forcing function.

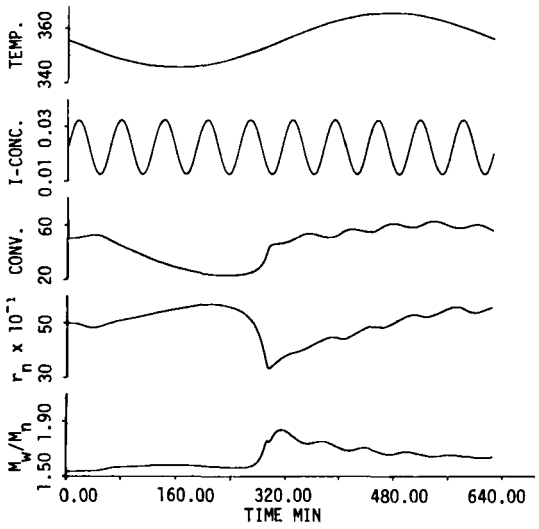

FIG. 4. Reactor dynamics (Run 13) for combination forcing function.

live polymer concentration, number-average chain length, and polydispersity are plotted against time. In less than two hundredths of a minute the two models approach the same values. Thus the PSSA appears to be valid for this system except for very short time periods just after reactor conditions are changed. Incorporation of the PSSA allows a larger time step size to be used, thus reducing machine computation time by a factor of about 20.

Test runs using periodic forcing functions again gave equivalent time averaged results with and without the PSSA. Thus this assumption was incorporated into the balance of the work reported in this paper.

PERIODIC OPERATION

The inlet initiator concentration and jacket temperature were forced separately and in combinations in square and sine wave forms. The effect of frequency, amplitude, and phase lag were surveyed.

The general form of the forcing function, F, was

$$F = Fs + F(t) \tag{10}$$

where Fs is the optimum steady-state value and F(t) is the periodic disturbance about the steady-state value.

Using the optimum steady-state conditions for the first case (Table 7) as the base, the effect of periodic operation was determined. The results are tabulated for the sine wave forms in Table 9 and for the square wave forms in Table 10. The performance indices listed are time averaged values for a holding time of 628 min.

Clearly, the time-averaged polydispersity could only be increased from the optimum steady-state value. Values of the time-averaged number-average chain length and percent monomer conversion were

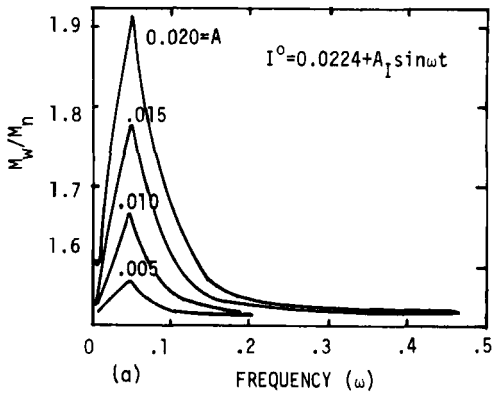

FIG. 5a. Frequency-amplitude diagram: M_w/M_n variations.

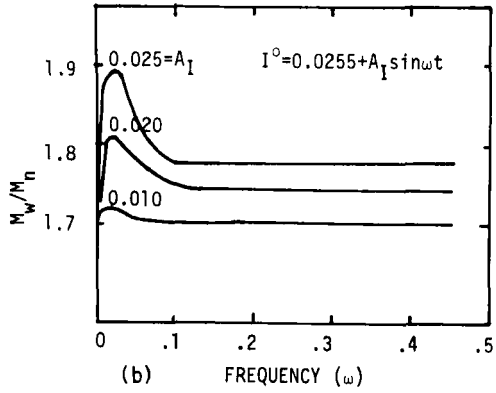

FIG. 5b. Frequency-amplitude diagram: M_w/M_n variations.

obtained both above and below the optimum steady-state values (although outside the imposed constraints in some cases). The effect of phase lag which was used in the studies with combination forcing functions appeared to be minor. The square wave form did produce slightly more change in reactor performance than the sine wave form.

Typical plots of the reactor performance for the specified holding time of 628 min are shown in Figs. 2-4.

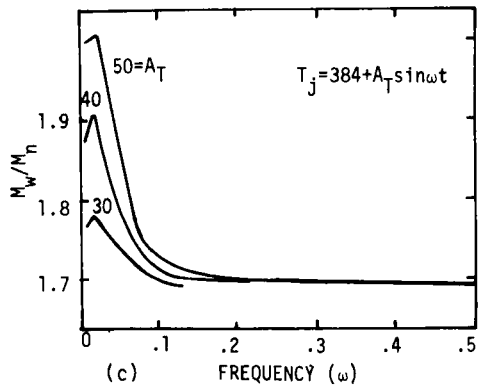

FIG. 5c. Frequency-amplitude diagram: M_w/M_n variations.

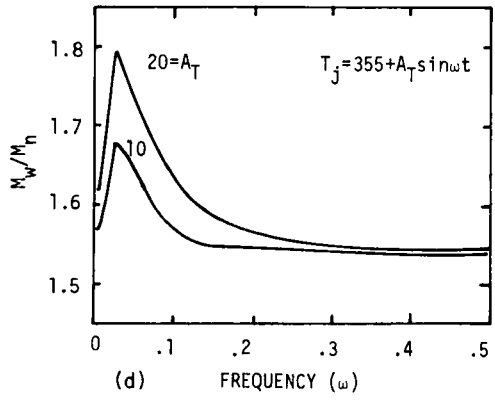

FIG. 5d. Frequency-amplitude diagram: M_w/M_n variations.

The effect of amplitude and frequency on the performance indices for the optimization problems with single sine wave forcing functions on inlet initiator concentration and jacket temperature is shown in Figs. 5-7.

Strong resonance behavior is shown in the polydispersity plots (Figs. 5a-d) with a maximum occurring at low frequencies. The effect becomes more pronounced with increase in amplitude. Minimums are shown in the number-average chain length diagrams (Figs. 6a-d) with mixed behavior in the percent monomer conversion plots (Figs. 7a-d).

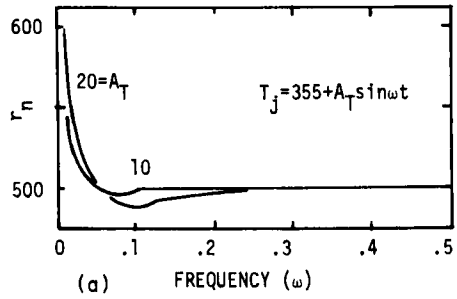

FIG. 6a. Frequency-amplitude diagram: number-average chain length variations.

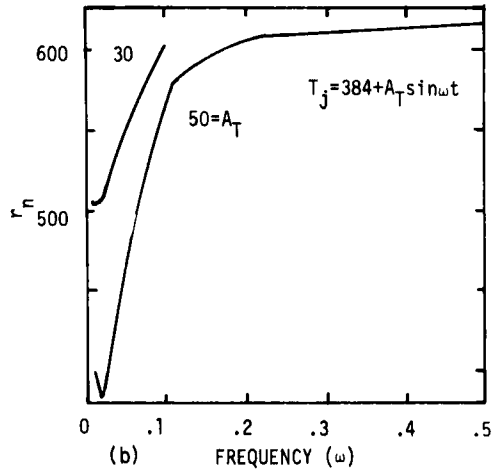

FIG. 6b. Frequency-amplitude diagram: number-average chain length variations.

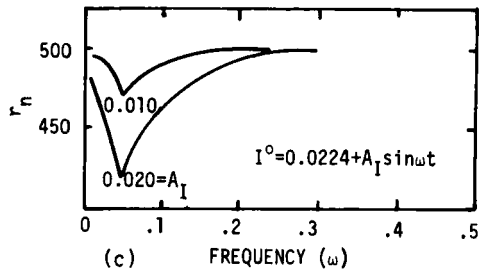

FIG. 6c. Frequency-amplitude diagram: number-average chain length variations.

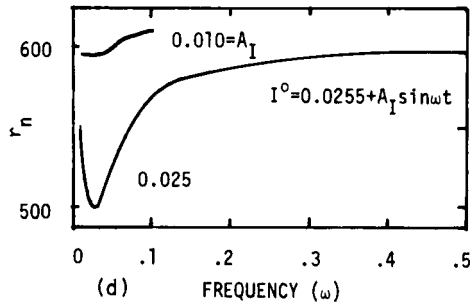

FIG. 6d. Frequency-amplitude diagram: number-average chain length variations.

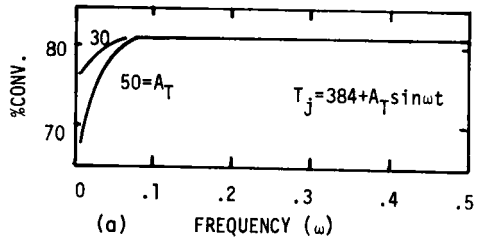

FIG. 7a. Frequency-amplitude diagram: monomer conversion variations.

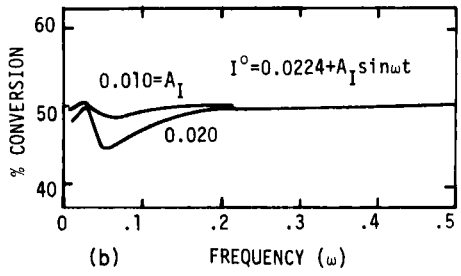

FIG. 7b. Frequency-amplitude diagram: monomer conversion variations.

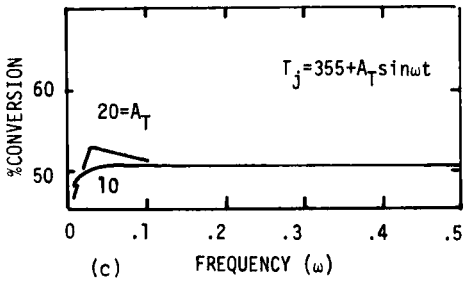

FIG. 7c. Frequency-amplitude diagram: monomer conversion variations.

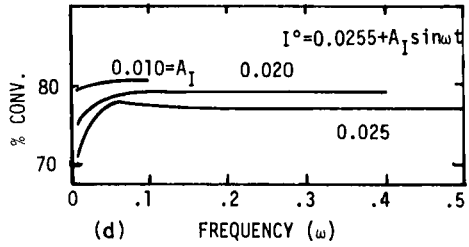

FIG. 7d. Frequency-amplitude diagram: monomer conversion variations.

CONCLUSIONS

Deliberate oscillations in selected forcing functions do appear to alter the reactor performance for the system studied. The most consistent effect is an increase in polydispersity at low frequencies, with the effect amplified with increase in amplitude. Thus this approach offers an alternate scheme for manipulating polymer properties. Implementation would be relatively simple as compared with, say, adding additional chemical components to achieve the same goal. Conversely, these results may indicate to a processor that he may want to eliminate uncontrolled oscillations in key operating variables to avoid producing undesirable polymer properties and conversions.

ACKNOWLEDGMENTS

The work reported in this paper was supported by grants from the Research Corporation, National Science Foundation (GK-32680) and Arizona State University Grants Committee.

REFERENCES

[1] W. H. Ray, Ind. Eng. Chem., Process Des. Develop., 7, 422 (1968).
[2] V. F. Bandermann, Angew. Makromol. Chem., 18, 137 (1971).
[3] J. P. Bianchi, F. P. Price, and B. H. Zimm, J. Polym. Sci., 25, 27 (1957).
[4] R. L. Laurence and G. Vasudevan, Ind. Eng. Chem. Process Des. Develop., 7, 427 (1968).
[5] A. Hui, M.S. Thesis, McMaster University, 1967.
[6] M. A. Bamford et al., The Kinetics of Vinyl Polymerization by Radical Mechanisms, Academic, New York, 1958.
[7] E. I. Jury, Theory and Application of the Z-Transform, Wiley, New York, 1964.

[8] D. W. Marquardt, J. SIAM, 11, 431 (1964).
[9] J. L. Kuester and J. H. Mize, Optimization Techniques with FORTRAN, McGraw-Hill, New York, 1973.
[10] B. Carnahan, H. A. Luther, and O. Wilkes, Applied Numerical Methods, Wiley, New York, 1969.
[11] L. P. Meissner, ZAM (Zonneveld-Adams-Moulton) Integration, Lawrence Radiation Laboratory, Berkeley, California, 1965.
[12] IBM System/360 Scientific Subroutine Package Version III, International Business Machines Corp., 1968.
[13] J. M. Box, Computer J., 8, 42 (1965).

Accepted by editor October 22, 1973
Received for publication December 19, 1973